

Chapter 6

Optimized Circular RFID Tag Antenna Achieving Extended Detection Range on Metallic Surfaces

6.1 Introduction

Radio frequency identification technique (RFID) has been utilized to accelerate the identification process as well as escalate the product management efficiency in different industries. The property of having high reading speed and range with tag at distant position has increased its demand and attracted researcher to explore in this captivating field. An RFID system consists of tags/transponders, reader and computer database. While inaugurating RFID tag design, the main aim is generally placed on outlining high performance tag with suitable application. The tag antenna receives power from incoming electromagnetic waves coming from the reader which is also sometimes referred as interrogator. The tag transforms this EM wave into electrical signal for Application Specific Integrated Circuit (ASIC) to activate itself [84]. The performance of tag antenna is determined by its potential to produce complex conjugate impedance to that of ASIC. Since, the tag is physically fixed to the item to trace, different antenna parameters like operating frequency, radiation

pattern, input impedance can vary according to the surface of the item.

In recent years, several papers were proposed on RFID tag for metallic objects. Frequency reconfigurable antenna[85], planar inverted-S antenna (PISA) accompanied by integrated U-shaped arm[86], omnidirectional tag having planar inverted-L antenna (PILA) [87], Loop antenna[88, 89, 90, 91], circular patch antenna[92, 93, 94, 95, 96], additionally antenna made up with specific designed structure, for instance one made with cavity type structure[97], are the most regularly used patterns for antennas to be used for on-metal RFID tag design to mitigate the problem of interference prompted by metal objects. However, in linearly polarized antenna, detection range decreased with the use of metal as well as the orientation of tag. Hence, it is advantageous to develop a novel antenna with circular polarization which can overcome the problem of mounting antenna on metal surface and its orientation.

Since, majority of UHF RFID system practise linearly polarized tag antenna[98, 99], circularly polarized tag antenna is put to employ for reader exercise to expand the reliability of spotting the arbitrarily aligned tag antennas[100, 101, 102, 103, 104, 105]. On account of polarization mismatch, only fifty percent of transmitted power from circularly polarized (CP) reader antenna is received by linearly polarized tag antenna. This mismatch can be improved by using CP tag antenna instead of linearly polarized tag antenna[106]. Reasonably, the maximum detection range of RFID system with CP tag antenna can be enhanced by 41% in contrast to that of LP tag antenna as 3 dB of more power is received in case of CP tag antenna.

Microstrip patch antennas have been engaged for the use of representing metallic RFID tags repeatedly. In this chapter, a pair of sectorial patches is engaged for the use of designing simple structure rather than complex structure. One of the L-shaped load bar is stub shorted with ground plane on rear side to lower the resonating frequency in the desired band. The L-shaped load bars provides impedance matching of the tag in the allocated UHF RFID band. It will be revealed further that inductive and capacitive loading effect of the introduced vias, L-shaped load bars and V-shaped slots are predominant in toppling the self resonating frequency of circular tag to the functional RFID UHF band.

The further section of the chapter is put in subsequent way. The configuration and design of circular tag antenna is discussed in Section 6.2, along with simulated results and generalised equivalent circuit diagram. The evolution steps of tag design with each step result is represented in Section 6.3. Section 6.4 analyzes the parametric analysis. The simulated and measured results are discussed in Section 6.5. Eventually, Section 6.6 concludes the chapter with the summary of major contributions of this research work.

6.2 Circular antenna design

The prime focus in designing tag antenna for metal tag is to diminish the interference from metallic surface. This purpose can be achieved by inserting high permittivity substrate or by introducing a High-Impedance surface[107]. A substitute method for this purpose is to introduce a metallic ground plane in the antenna layout in order to diminish the repercussion of metal surface on the characteristics of the antenna[108]. In this chapter, authors have introduced a looped-circular non-planar RFID metallic tag design. Fig. 6.1 shows geometry with parameters as well as the 3-D view of proposed antenna. This presented CP circular tag antenna has radius of 34mm. The geometrical parameters and their values are shown in Table 6.1.

The antenna is made up of a pair of sectorial patch on top and comprises two symmetrical

Table 6.1: Geometrical parameters of circular tag antenna

Parameter	Value(mm)	Parameter	Value(mm)
a	6.3	b	9.8
c	11.31	d	2.2
w	1.7	p	5.5
l_s	22.62	l_p	28.28
s	18.4	r	0.5

L-shaped load bars on top in slot region. The tag antenna comprises a metallic plane at bottom also. The bottom plane is connected with patch through 7 vias at each side to form a loop antenna. The a shorting pin was introduced inside L-strip. A circular polarization is generated by a composite radiating element consisting of an electric L-shaped thin metal strip and a magnetic slot cut in an arc-shaped top metal piece. These orthogonal electric

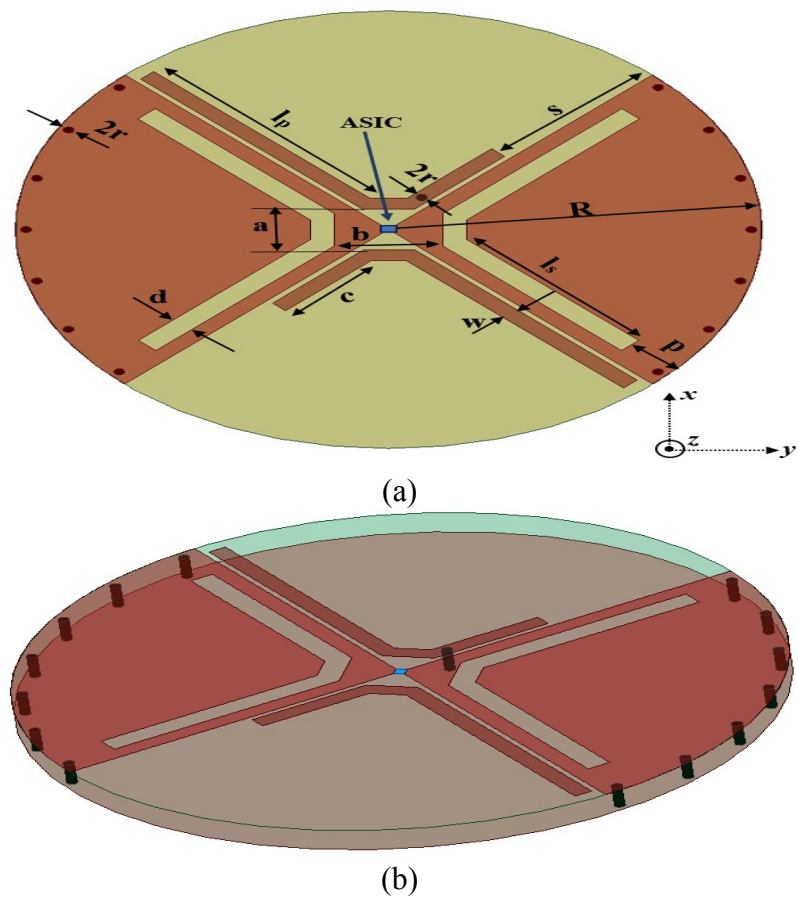


Figure 6.1: Structure of proposed circular RFID tag antenna. (a) Dimensional geometry. (b) 3-D view.

and magnetic radiators exhibit a 90-degree phase difference [109]. The L-strip and slots are half-wavelength long, with a shorting-pin introduced to achieve the required quadrature phase relationship. The ASIC is attached across aperture between two arc-patches and touches both of them. Simulated results of circular CP tag antenna is shown in Fig. 6.2. The simulated input impedance of tag antenna and ASIC at 909 MHz with value of $16.3 + j278.6\Omega$ and $12.6 - j279\Omega$ respectively, is shown in Fig. 6.2(a). The reflection coefficient of tag was obtained below 10 dB between 900 MHz and 918 MHz with axial ratio below 3 dB between 907 MHz and 920 MHz as displayed in Fig. 6.2(b). Simulated radiation pattern for x-z plane and y-z plane are shown in Fig. 6.2(c) and (d) respectively.

In the interest of validating the circularly polarized radiation at desired frequency,

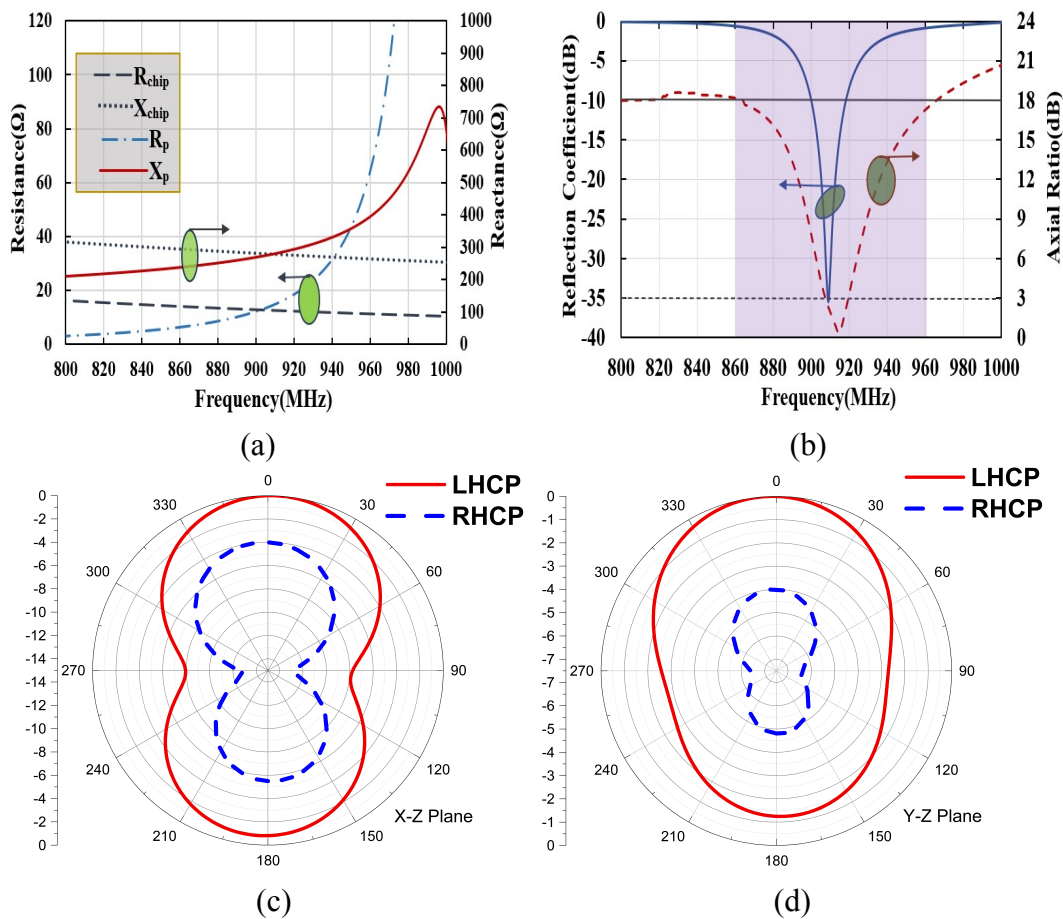


Figure 6.2: Simulated results of circular antenna (a) Input impedance, (b) Reflection coefficient and Axial ratio, (c) Radiation pattern for xz-plane, (d) Radiation pattern for yz-plane

simulated surface current distribution of the proposed circular tag antenna is illustrated at different phases 0° , 90° , 180° and 270° as displayed in Fig. 6.3. The rotation of cur-

rent direction validates the circular tag antenna to be LHCP antenna. In UHF RFID tag

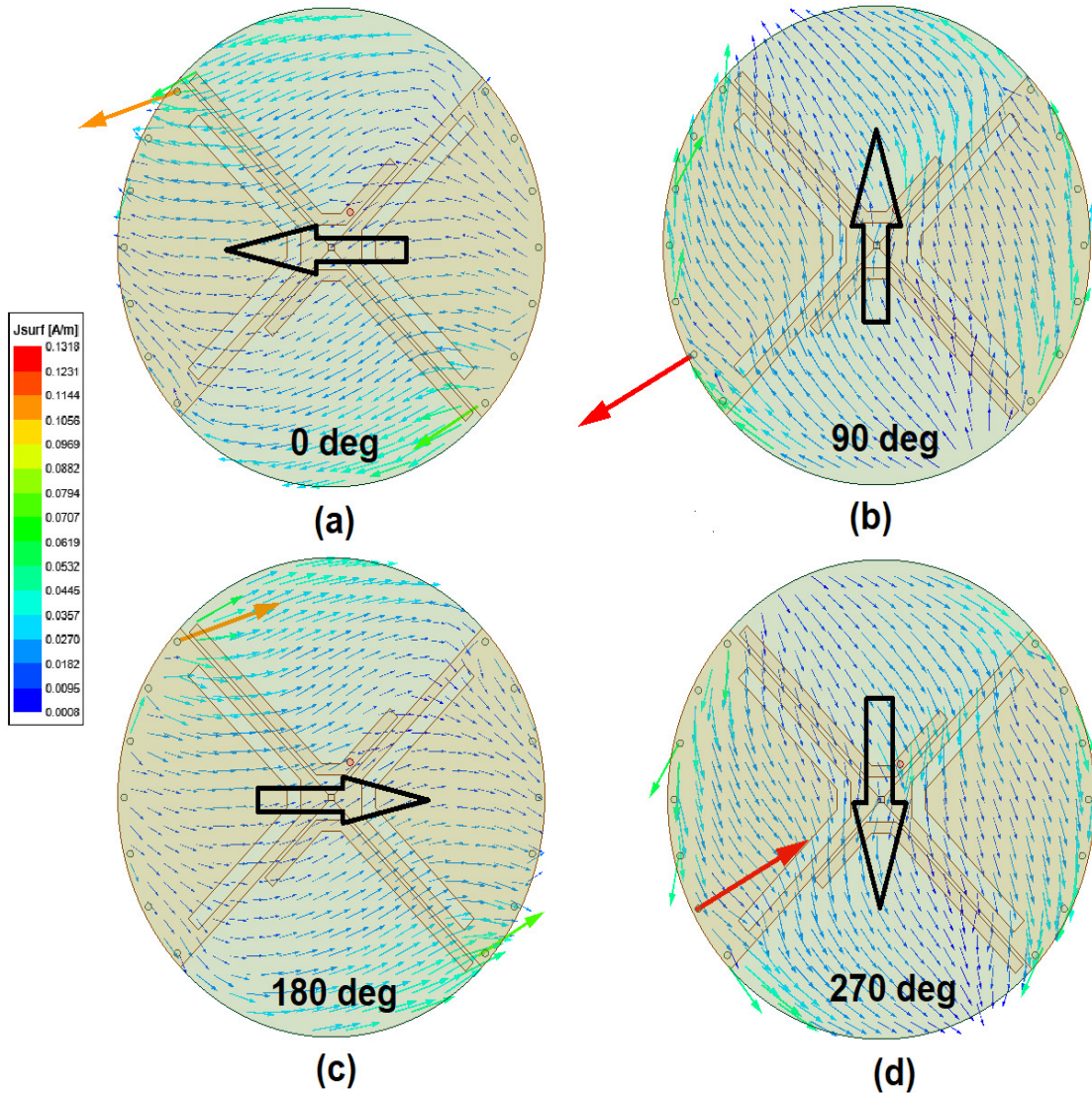


Figure 6.3: surface current density of circular tag antenna at 915 MHz at different phases. (a) $\omega t = 0^\circ$, (b) $\omega t = 90^\circ$, (c) $\omega t = 180^\circ$, (d) $\omega t = 270^\circ$

delineation, the important subject is to alter the resonating frequency in UHF band with desired complex inductive impedance of antenna[110]. This fundamental theory provides the key to a perception of RFID tag delineation and will be utilized to elaborate the concepts upon which this circular metal tag antenna built. A general and equivalent circuit diagram of proposed circular tag antenna is displayed in Fig. 6.4(a) and (b) respectively. The ASIC used in this article is NXP UCODE7 which contains an internal circuit of parallel combination of resistor R_{chip} and capacitor C_{chip} with values of 5.8 k Ω and 0.63 pF respectively. Every via introduces analogous inductor L_{viaN} , L-bars introduce inductance

L_{bar} and capacitance C_{bar} , V-slots introduce capacitance C_s and R_r is total resistance of radiating body in general circuit version of tag antenna.

The resonating frequency of circular tag antenna can be expressed as $f_o = 1/(2\pi\sqrt{L_{eq}C_{eq}})$,

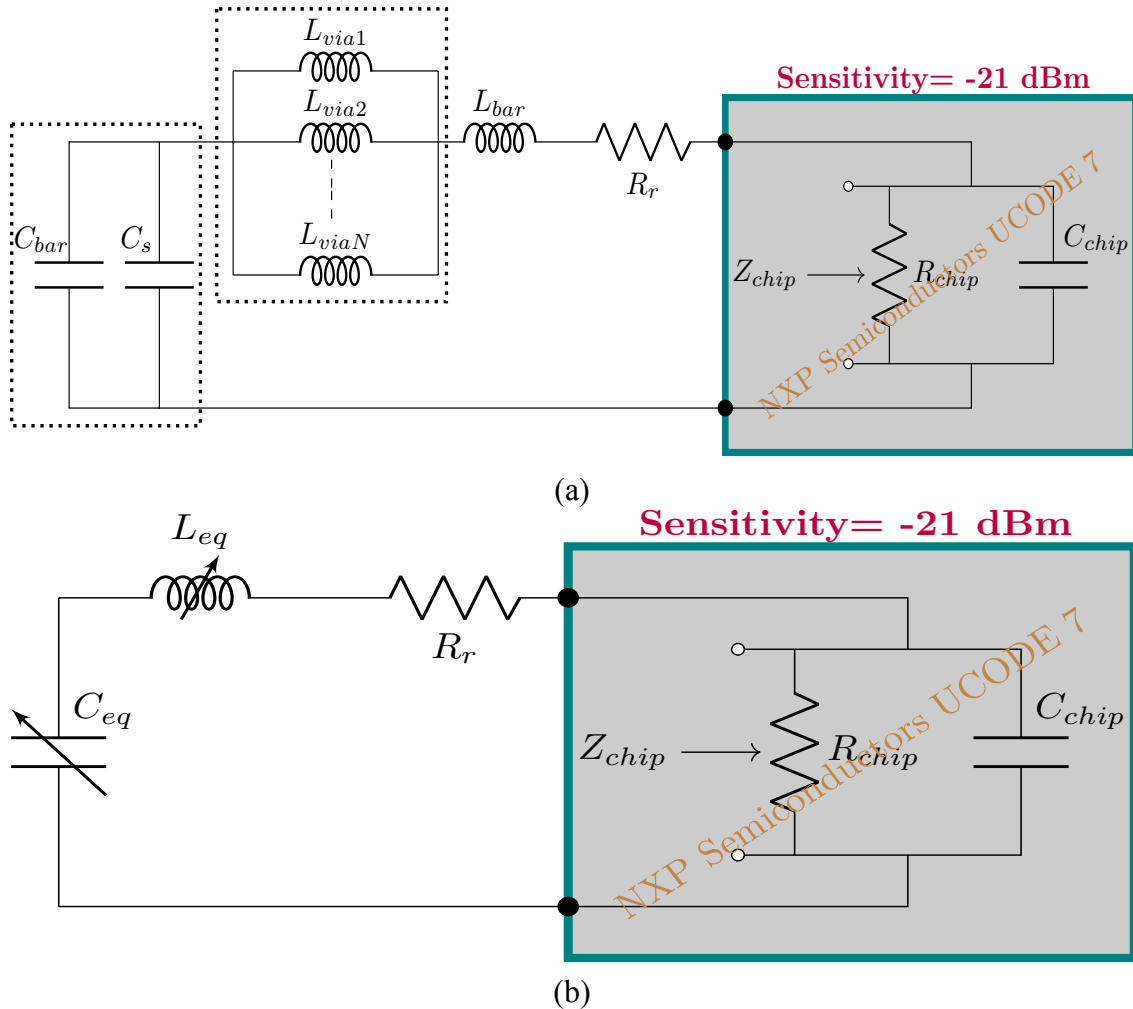


Figure 6.4: Circuit representation of proposed Circular RFID tag antenna. (a)General circuit version. (b) Equivalent circuit diagram.

where, L_{eq} and C_{eq} are the equivalent inductance and capacitance respectively of circular tag antenna displayed in Fig. 6.4(b). The values of L_{eq} and C_{eq} can be taken from Fig. 6.4(a). The resonating frequency f_o can be managed by tuning either equivalent inductance or equivalent capacitance of tag antenna.

Initial Design and Optimization Strategy: The antenna layout begins with a circular configuration that utilizes a pair of sectorial patches and L-shaped load bars to achieve compact size and polarization control. Instead of relying on traditional resonant-length guidelines, the structure was initially shaped to accommodate circular symmetry and fa-

avorable surface current rotation. The design includes a V-slot and L-shaped sectorial patches placed to achieve circular polarization. Initial dimensions were selected based on theoretical resonator models, with the patch area roughly matching half-wavelength criteria. The shorting pin, slot width, and spacing between L-bars were systematically varied to achieve axial ratio below 3 dB and ensure impedance matching. The use of vias and slots helped fine-tune the resonance and polarization properties. The final geometry (Table 6.1) was determined through simulations that minimized reflection coefficient and optimized axial ratio bandwidth.

6.3 Evolution steps of Circular CP loop tag antenna

In this section, proposed tag antenna is studied and correlated. The proposed CP looped metal attachable planar RFID tag antenna is fabricated on a FR4 substrate with thickness of 3.2mm, dielectric constant of 4.4 and loss tangent of 0.02. The evolution steps of final designed tag is shown in Fig. 6.5(a)-(d). The ASIC is introduced in the centre of circular tag antenna.

A symmetrical pair of sectorial slot and patch is imbedded in circular tag as shown in

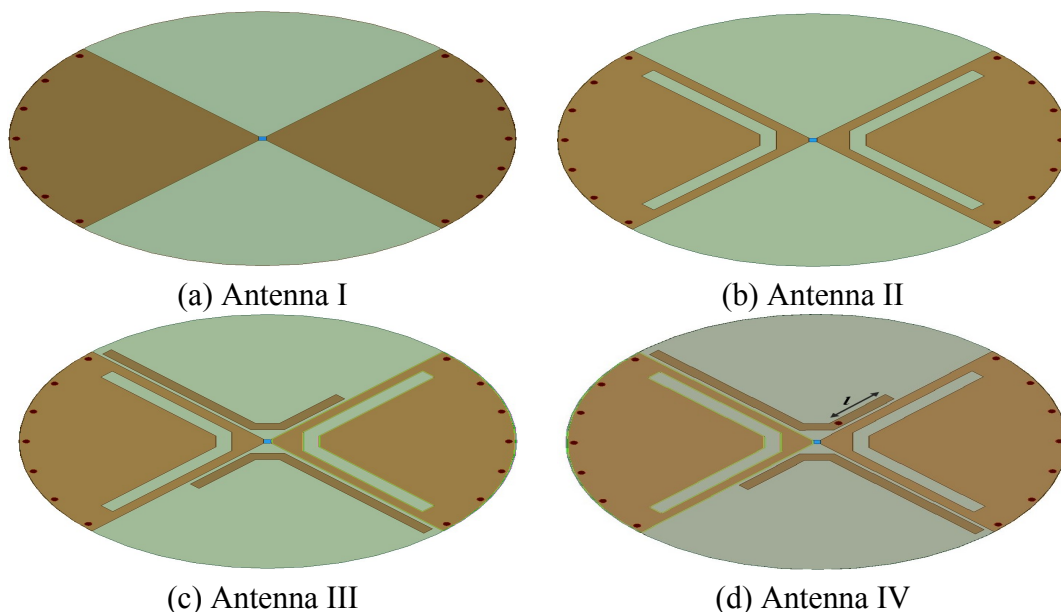


Figure 6.5: Evolution steps (a) pair of slot and patch with equal area,(b) V-shaped slot,(c) L-shaped patch,(d) shorting pin in L-patch.

Fig. 6.5(a). The vias are introduced at ends to make it a loop antenna and introducing CP

radiation. However, this loop antenna shows very poor reflection coefficient. Further, a pair of V-shaped slot is embedded inside the sectorial patches as shown in Fig. 6.5(b). The slot introduces capacitive effect and causes resonating frequency to shift in lower band. Further, to shift resonating frequency in UHF band, a pair of L-shaped bar is embedded in sectorial slots as shown in Fig. 6.5(c). Further, a shorting pin is introduced inside L-shaped load bar at a distance of $l = 10mm$ from ending terminal of L-bar as shown in Fig. 6.5(d). It connects the load bar with ground plane and introduces resistance and inductance in tag so that the tag impedance becomes complex conjugate of ASIC.

The simulated input impedance is shown in Fig. 6.6(a) for each step of circular tag antenna. The reflection coefficient and boresight Axial ratio obtained at each step is shown in Fig. 6.6(b). From Fig. 6.6(b), it can be seen that resonance frequency from Antenna II to III shifts to lower value because of increase in equivalent capacitance, therefore capacitance introduced by L-bar and V-slot are parallel with each other in Fig. 6.4(a).

6.4 Parametric Analysis

6.4.1 Effect of vias

In the design, every pair of via is analogous to single-loop formation and hence can be viewed as single inductor. Thus, multiple pairs of vias are analogous to multiple inductors $L_{via1}, L_{via2}, L_{via3} \dots L_{viaN}$. The effect of various pairs of vias on input impedance is displayed in Fig. 6.7. It is noticeable that as the number of via pairs get larger, it tends to decrease the inductance values and thereby self-resonating frequency $f_{o,via}$ shifts to higher values. Thus, all the via inductors serves to be in parallel as shown in Fig. 6.4(a). It is noticeable that if we increase number of vias above a certain limit, the self-resonating frequency shifts beyond the UHF band of RFID system. In the light of this, seven pairs of vias have been chosen to design the circular tag which has been presented in this paper.

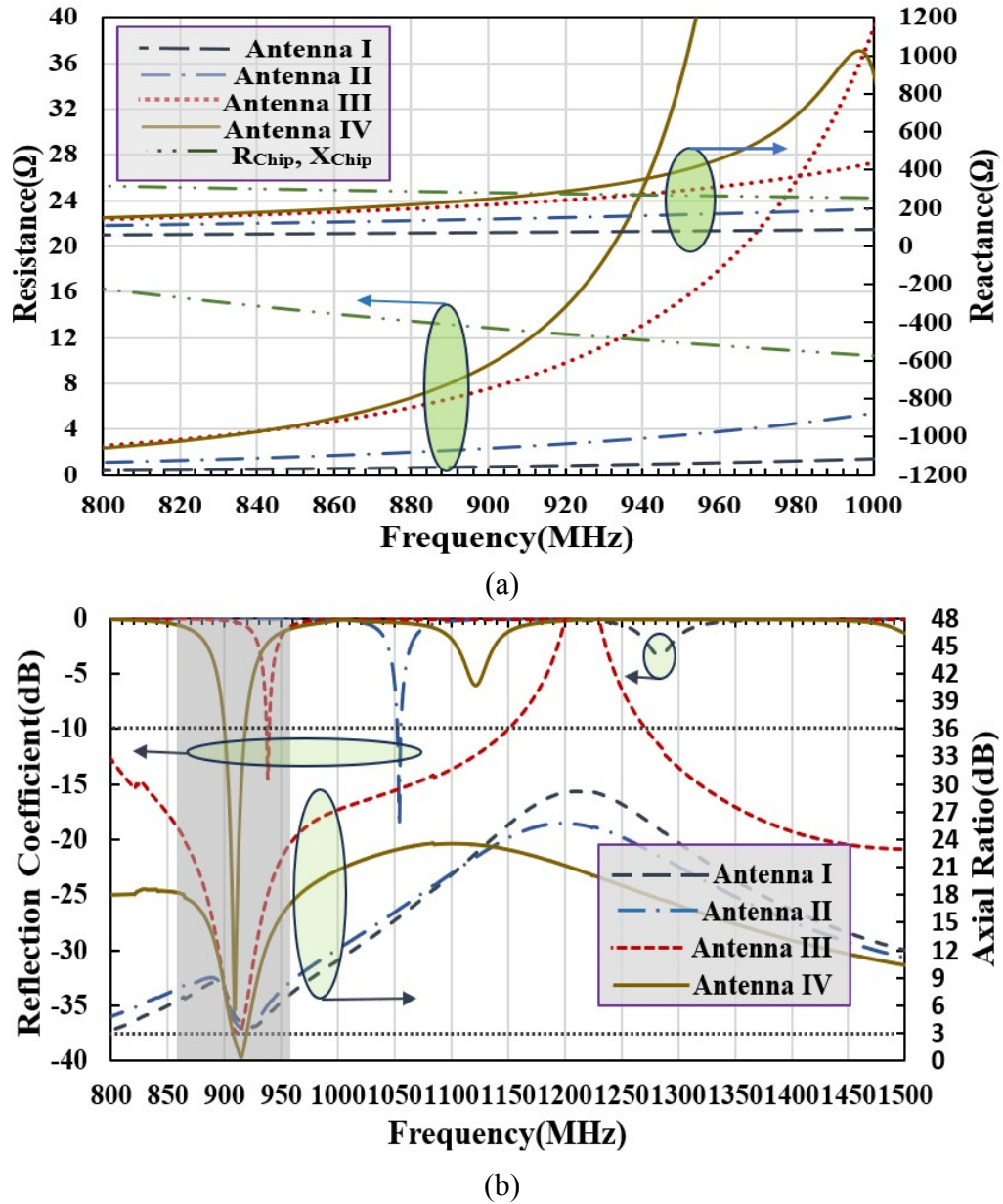


Figure 6.6: Simulated results of Circular tag antennas: (a) Input impedance variation, (b) Reflection Coefficient and axial ratio.

6.4.2 Effect of gap between L-shaped patches

In this chapter, authors have introduced two L-shaped load bars to be essential parts of metallic circular tag antenna which are placed along but not connecting the arc shaped patch. The effect of distance between both load bars is shown in Fig. 6.8. Effect of separation was analyzed for impedance values at 5.3mm, 6.3mm, 7.3mm and 9.3mm. It is observed that by increasing the separation between bars, self-resonating frequency is shifted towards higher values. However, if load bars are separated beyond some value,

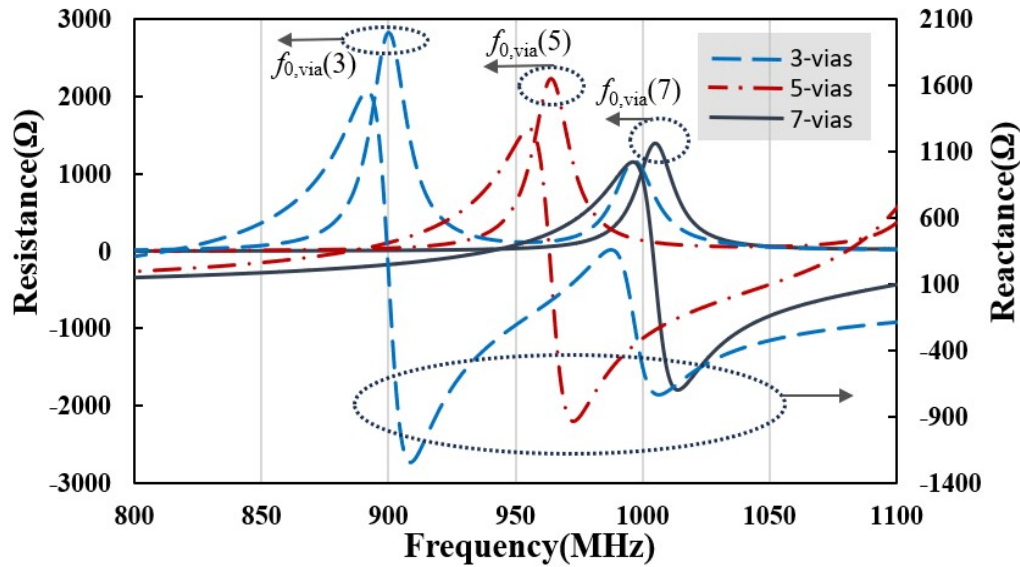


Figure 6.7: Self resonating frequency of circular tag with different amount of pair of via.

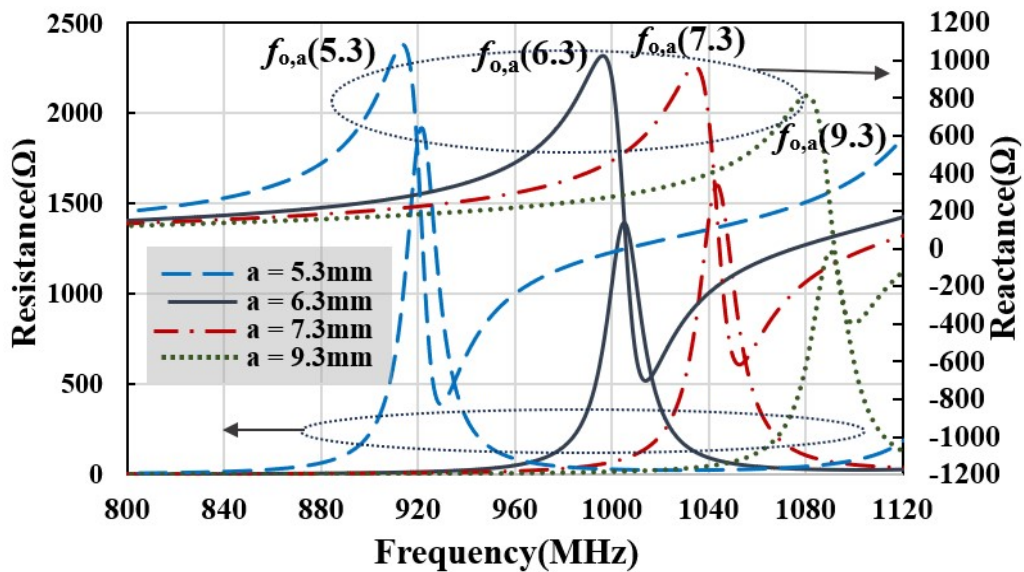


Figure 6.8: Effect of distance between L-bars in circular tag.

the self-resonating frequency shift beyond Ultra High Frequency Band for RFID systems. Additionally, these L-shaped bars also contribute capacitance C_{bar} of the circular metal tag antenna. So, by regulating their parameters give rise to way for tuning the antenna. This characteristics is very helpful for the viewpoint of designers endeavouring to optimize the characteristics of circular metal tag antenna.

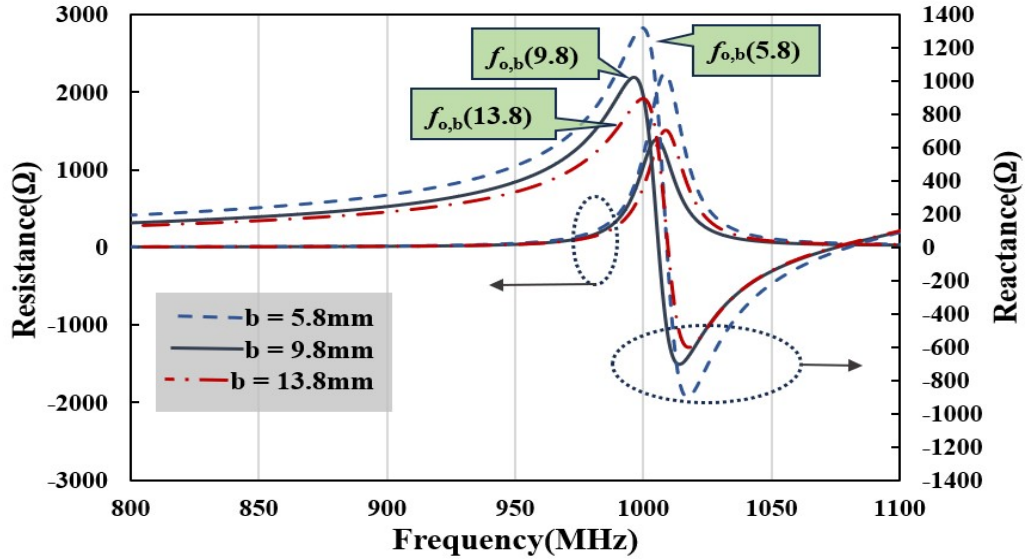


Figure 6.9: Effect of gap between V-slots in circular tag.

6.4.3 Effect of gap between V-shaped slots

The dominating capacitance C_s of circular tag antenna varies with the gap between slots inside sectorial patches as shown in Fig. 6.9. As the gap increases, reactance of tag decreases. This implies the capacitance in tag decreases with the gap and hence resonating frequency $f_{o,b}$ increases. Thus, f_o can not only be controlled by number of vias in arc-patch but also gap between V-slots. However, for a fixed resonating frequency f_o , this gap, b , as well as the radius of circular tag antenna, R , can be increased to increase its effective inductance at the same time. By using larger antenna size, we can achieve higher gain and thus it can achieve higher detection range need for RFID tag placed on metallic gadgets.

6.4.4 Effect of shorting pin position on Axial ratio

Fig. 6.10 shows the simulated boresight axial ratio as a function of l . It can be seen that increasing value of l shifts axial ratio at higher frequency. This parameter plays important role in achieving good axial ratio bandwidth within operational band of the presented circular tag antenna.

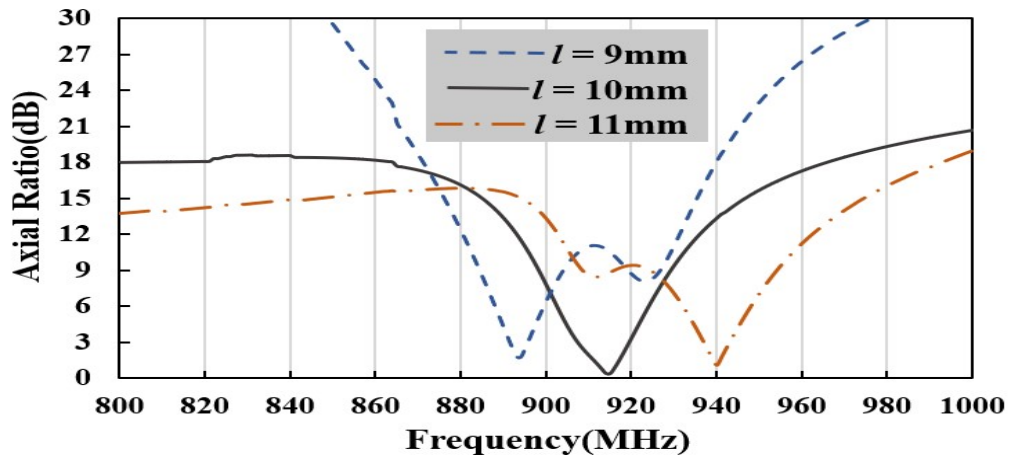


Figure 6.10: Effect of shorting pin position on axial ratio.

6.5 Results and Analysis

After finding the simulated results, the circular antenna input impedance measurement was done by using a differential probe, two test cables and a Vector Network Analyzer. In the process, VNA was first calibrated and then circular tag antenna which was connected with differential probe, was connected to VNA using two test cables of the VNA. Then port extension technique was used to shift the calibration plane to measurement plane of circular tag antenna. Thus, the S-parameters were measured by VNA. After that, antenna impedance was calculated by using equations given in eq. 6.1.

$$Z_{in} = 2Z_0 \frac{(1 + S_{12}S_{21} - S_{11}S_{22} - S_{12} - S_{21})}{(1 - S_{11})(1 - S_{22}) - S_{21}S_{12}} \quad (6.1)$$

Tag antenna impedance measurement setup was done in anechoic chamber with $310 \times$

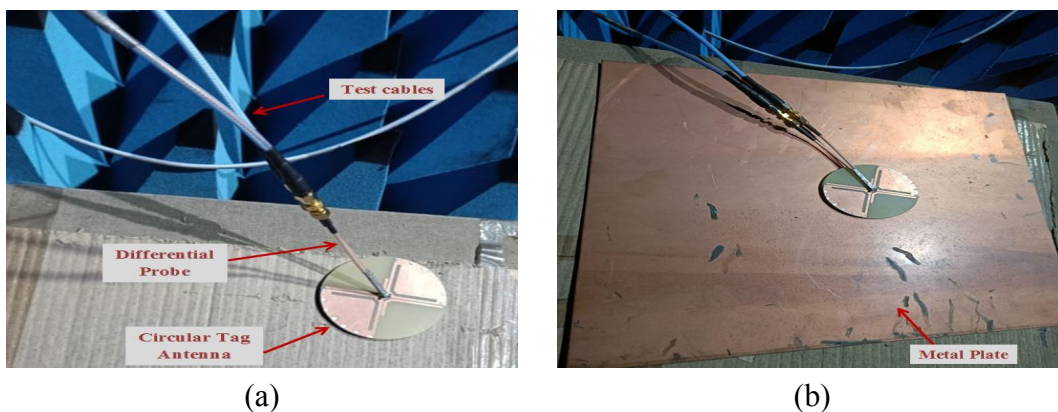


Figure 6.11: circular tag antenna measurement setup (a) without metal plate and (b) with metal plate.

310 mm² metal plate and without metal plate as shown in Fig. 6.11(a) and (b). Impedance measurement was done with Anritsu MS2038C Vector Network Analyzer. The simulated and measured antenna impedance is shown in Fig. 6.12. The complex conjugate with

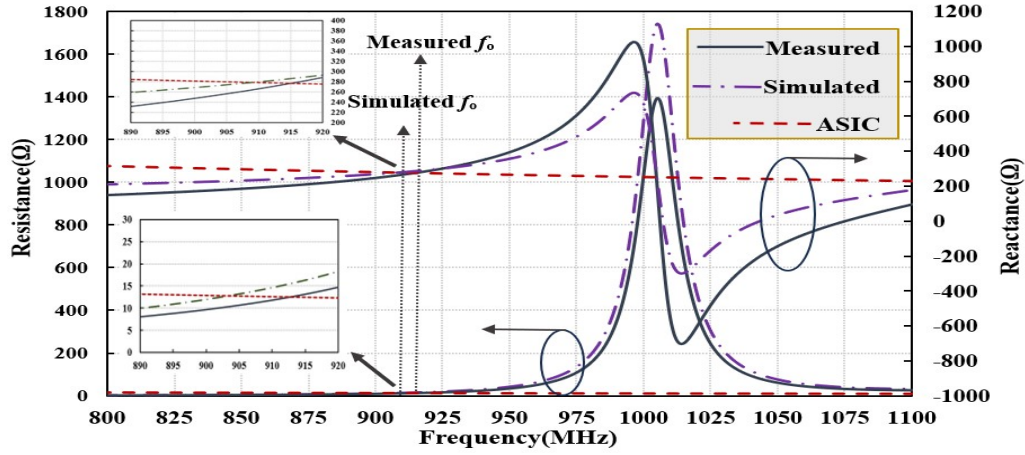


Figure 6.12: Simulated and measured impedance of circular tag antenna in UHF RFID band.

NXP Ucode 7 ASIC is obtained at 915 MHz. The ASIC used in this work exhibits internal input impedance of $12.5 - j277 \Omega$ at 915 MHz. The measured input impedance of circular tag found to be $13.1 + j276.95 \Omega$ at matching resonant frequency of tag. However, the measured impedance matching is obtained 6 MHz higher than that of simulated result. This slight discordance of impedance matching can be associated to error in port extension and antenna manufacturing imperfections. Reflection coefficient of the circular tag antenna is obtained by eq. 6.2.

$$\Gamma = \frac{Z_{chip} - Z_a^*}{Z_{chip} + Z_a} \quad (6.2)$$

where, $Z_{chip} = R_{chip} - jX_{chip}$ and $Z_a = R_a + jX_a$ are impedance of ASIC and circular tag antenna respectively. Reflection coefficient of tag antenna was obtained with metal plate and without metal plate. The measured reflection coefficient without metal plate was found below 10-dB between 906 MHz and 923 MHz. Tag antenna was also simulated with $310 \times 310 \text{ mm}^2$ metal plate to see the difference. It can be seen from Fig. 6.13 that there is no significant change in reflection coefficient of tag when placed on metal plate, hence this circular tag antenna can be attached to metallic round surface such as metallic rotating shafts wherever applicable for detection. The maximum detection range of circular tag

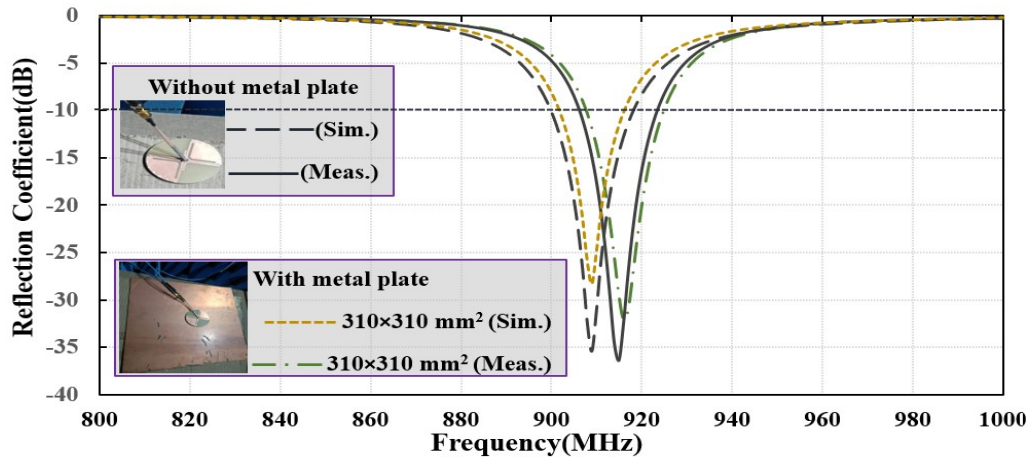


Figure 6.13: Reflection coefficient of circular tag antenna with and without metal plate.

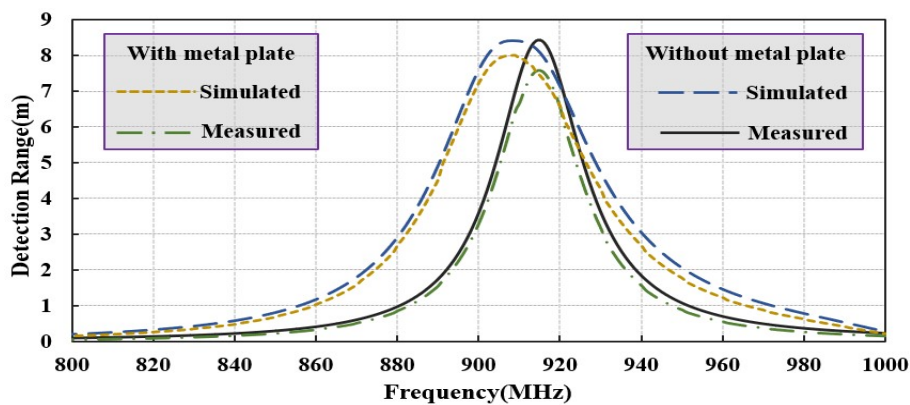


Figure 6.14: Maximum detection range of proposed circular tag CP antenna.

antenna was evaluated by eq. 6.3.

$$D_{max}(\theta, \phi) = \left(\frac{\lambda_0}{4\pi} \right) \sqrt{\frac{EIRP_R}{P_{th,chip}} (1 - |\Gamma|^2) G_t(\theta, \phi)} \quad (6.3)$$

where, λ_0 is wavelength, $EIRP_R$ is 4W EIRP transmitting reader power and $G_t(\theta, \phi)$ is gain of circular tag antenna. This circular tag antenna realized a good simulated gain of -6.77 dBic at boresight. The sensitivity, $P_{th,chip}$ is -21 dBm. The simulated and measured detection range at the boresight are displayed in Fig. 6.14 with maximum detection range of 8.42 m when simulated without metal plate. Detection range was found for both the cases i.e. when tag was on the metal plate and when tag was not on the metal plate. Boresight maximum detection range obtained in each case is shown in Table 6.2, which describes that there is not significant effect of metal plate on tag.

Table 6.2: Read Range Comparison in Different Conditions

Condition	With Metal Plate (m)	Without Metal Plate (m)
Simulated Detection Range	7.9	8.420
Measured Detection Range	7.58	8.422

Table 6.3 displays the comparison between proposed circular tag CP antenna and some of other proposed CP rectangular tag antenna for UHF RFID. Proposed circular tag is compared in terms of operating frequency, polarization characteristics, used substrate, measurement with metal plate, reflection coefficient bandwidth, Axial ratio bandwidth and maximum detection range with metal-attachable tags except [103]. It can be seen the trade-off between 10-dB reflection coefficient bandwidth and 3-dB axial ratio bandwidth. However, proposed circular tag has axial ratio below 3 dB bandwidth is highest among others except [104]. This proposed metal-attachable tag can be detected from practicably extended range of more than 8 meters. The presented tag antenna is circular in size while other tag antennas are rectangular in shape which makes it a novel tag antenna with long reading range.

Table 6.3: Comparison of different CP tag RFID antenna

work	Freq. (MHz)	Polarization	Substrate	Measured with metal plate	10-dB S_{11} BW	3-dB AR BW	Simulated Gain(G_t)	Detection range (m)
[96]	915	CP	FR4	No	40 MHz	6 MHz	-13.3 dBic	5.05
[102]	925	CP	FR4	No	50 MHz	6 MHz	-14.4 dBic	4
[103]	910	CP	Roger	No	37 MHz	11.4 MHz	-14 dBic	7.6
[104]	915	CP	FR4	No	25 MHz	20 MHz	-8.45 dBic	4.25
[105]	914	CP	FR4	No	31 MHz	6 MHz	-11.4 dBic	4.7
[111]	911	CP	FR4	Yes	60 MHz	12 MHz	-13 dBic	4.36
[112]	915	CP	FR4	No	100 MHz	6 MHz	-6.2 dBic	5.08
This work	915	CP	FR4	Yes	17 MHz	13 MHz	-6.77 dBic	8.4

6.6 Outcome

In this article, a novel circularly polarized metal-attachable UHF circular RFID tag antenna is presented. The vias present in tag boundary make it loop antenna with circular polarization. Equivalent circuit diagram is also presented. The evolution steps how proposed structure operates in desired frequency band and have complex conjugate of impedance of the ASIC. Further, parametric analysis was done to understand the effect of vias, gap of L-bars and gap of V-slots on resonating frequency of circular tag. Circular Tag antenna was fabricated and measured with metal plate and without metal plate. The experimental scrutiny have manifested that read range are in good agreement when placed on metal plate and when measured without metal plate.